Journal of Colloid and Interface Science 458 (2015) 32–38
Journal of Colloid and Interface Science

Solid-state encapsulation of Ag and sulfadiazine on zeolite Y carrier

Vesselina Mavrodinova[a], Margarita Popova[a], Krassimira Yoncheva[b], Judith Mihály[c], Ágnes Szegedi[c,⇑]

[a] Institute of Organic Chemistry with Centre of Phytochemistry, Bulgarian Academy of Sciences, 1113 Sofia, Bulgaria
[b] Faculty of Pharmacy, Medical University of Sofia, 2 Dunav Str., 1000 Sofia, Bulgaria
[c] Research Centre for Natural Sciences, Institute of Materials and Environmental Chemistry, Hungarian Academy of Sciences, 1117 Budapest, Magyar tudósok körútja 2, Hungary

G R A P H Y C A L A B S T R A C T

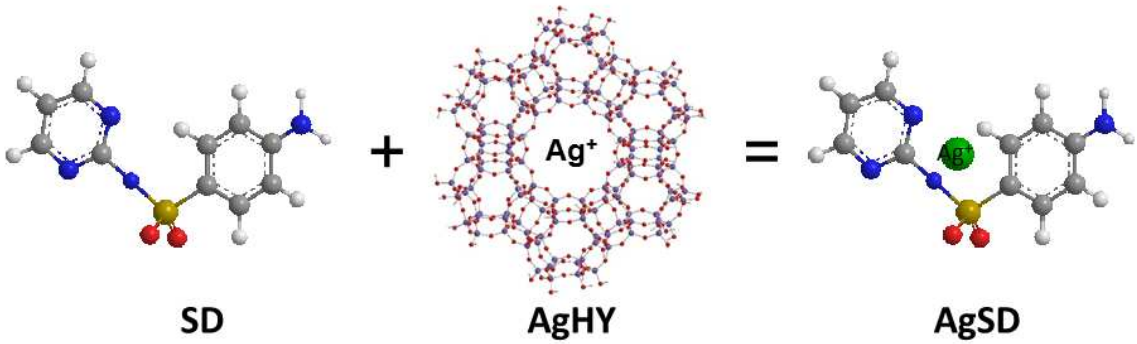

A B S T R A C T

Hypothesis: A new simplified procedure for encapsulation of antibacterial silver nanoparticles by Solid-state Ion Exchange (SSIE) procedure over zeolite Y, followed by deposition of sulfadiazine (SD) by dry mixing was examined for the preparation of topical antibacterial formulations. The ion-exchange and adsorptive properties of the zeolite matrix were utilized for the bactericidal Ag deposition and loading of antibiotic sulfadiazine.

Experiments: Assessment of the encapsulation efficiency of both active components loaded by solid and liquid deposition methods was made by X-ray diffraction, TEM, FT-IR spectroscopy and thermogravimetric analysis (TGA). SD release kinetics was also determined.

Findings: Sustained delivery of sulfadiazine has been observed from the Ag-modified zeolites compared to the parent HY material. It was found that if SD was loaded in solution, part of the zeolite silver ions was released and interacted with SD, forming AgSD. By solid-state SD deposition, the reaction between the drug and the silver was restricted within the limits of inter-atomic interaction, and total but prolonged drug release occurred.

1. Introduction

Silver nanoparticles are termed as new-generation of antimicrobials [1]. They have been recognized as excellent antimicrobial agents because of their effective biocide ability and nontoxicity to human cells [2–6]. According to Bonde et al. [7] the activity of standard antibiotics was significantly increased in the presence of silver nanoparticles and that can be used effectively against antibiotic-resistant pathogens.

A new aspect in searching for enhanced bactericidal effect for silver has been demonstrated in some researches on the synergistic effects of ionic silver with different antibiotics used in the treat- ment of burn wound infections [8,9]. Synergistic effects have also been demonstrated for chitosan–silver nanocomposites on strain of Staphylococcus aureus [10], for b-lactam antibiotics combined with silver nanoparticles and on strain of Escherichia coli [11]. However, no one of these silver containing combined systems have used zeolite materials as carrier.

The ion-exchange capability of zeolites might be used to load drug agents as well as to release them. The usage of zeolites as scaffolds for drug delivery is, however, relatively scarcely investigated. The substitution of silicon by aluminum atoms in the zeolite framework requires the presence of charge compensating counter-ions, usually H^+ or transition metal elements, which impart unique ion-exchange properties [12]. Because of these properties, they have been used to control release of supported silver species with bactericidal action and also for drug delivery in model systems [13,14].

There are several examples of biomedical applications of zeolites reported in the literature for wound treatment [15], herbicide release [16], and drug adsorption from polluted waters [13,18–22] including sulfonamide antibiotics [17–19]. Also, stable formation of hybrid assembly between zeolite (type L) and bacteria (E. coli) was realized and the exchange of specific information as well as the movement of the bacterium has become possible. Thus the authors developed an innovative potential phototherapeutic tool (De Cola [20–21]) able to target, label, and photoinactivate patho- genic and antibiotic-resistant bacteria.

Besides the traditional methods for drug encapsulation like adsorption from solution and incipient wetness impregnation, different approaches for drug loading in solid-state as physical mixing (wet paste), ball milling, high pressure homogenization in water, or wet media milling and spray-drying of the drug dissolved in its amorphous/nanocrystalline state on the support [22–26] could be employed.

In our previous papers drug formulations containing resveratrol supported on mesoporous silicas and zeolite (Y and BEA) carriers prepared by dry physical mixing in a vibrating ball mill mixer have been described [27,28]. Also, Ag modifications obtained by direct or post-synthesis methods for introduction of silver nanoparticles in MCM-41 and SBA-15 materials loaded with SD have been studied [27]. In the present publication, a solid-state encapsulation approach for introduction of both silver and sulfadiazine (SD) has been applied, utilizing the specific ion-exchange and adsorption properties of Y zeolite support. To the best of our knowledge no report on drug systems containing Ag and SD loaded together over a zeolite carrier have been published yet. Neither the preparation method, viz. solid-state ion exchange of Ag and subsequent mechanical deposition of sulfadiazine over Ag-loaded zeolite has been reported.

Solid state ion-exchange as a method for introduction of mono-, di- and polyvalent cations has some advantages over the conventional liquid ion exchange. By the solid encapsulation (i) handling of large volumes of salt solutions is not required; (ii) the problem of waste salt solution can be avoided and (iii) metal cations may be introduced into narrow pore cavities in such cases when the large hydration shell of the cations might prohibit the ion-exchange procedure in solution.

In the present work we attempt to apply this more facile, simplified and efficient formulation approach for preparation of drug delivery system containing both the antibiotic sulfadiazine and silver as a bactericide component. Commercial zeolite Y with high surface area and pore volume, as well as high ion-exchange capacity, was chosen as a support for drug loading by the consecutive solid-state procedures. The method developed by us, considering the ion-exchange ability of zeolites, made possible the formation of silver sulfadiazine (AgSD) as well. AgSD also offers many therapeutic advantages in topical use over other silver salts [30].

Drug amorphization by different nanosizing procedures, in particular the milling one, are widely used from the beginning of the nineties, as an efficient method to increase the drug solubility in water and dissolution velocity [22–26]. During the solidstate deposition of sulfadiazine, amorphization of SD crystals was also supposed to occur. In the present contribution a solid dispersion method was developed for the encapsulation of two medical con- stituents, such as SD and Ag, and it was compared with the more popular solvent deposition approach. The physico-chemical properties and the SD release kinetics in pH = 5.5 phosphate buffer over the H- and Ag-form Y zeolite carriers were also evaluated.

2. Experimental

2.1. Materials and methods

2.1.1. Zeolite Y carrier

Zeolite Y in its ammonium form was supplied by Zeolyst International (UWE Ohlrogge (VF), CBV 500) as a powder with the following characteristics: Si/Al molar ratio of 2.6, Na_2O = 0.2 wt.%, unit cell size = 24.53 Å, surface area (BET) = 750 m^2/g and total pore volume of 0.34 cm^3/g. The decomposition of the NH_4-form was performed by stepwise heating in dry N_2 as follows: heating up to 300°C, hold for 30 min and then heating from 300°C to 550°C, hold 90 min. The heating rate was 8 °C/min. The as-obtained parent material is designated as HY.

2.1.2. Host–guest system preparation. Ag and sulfadiazine loading

Solid-state encapsulation method has been used for the preparation of the following formulations: (i) parent HY zeolite loaded with SD only, designated as SD/HY(SS); (ii) parent HY loaded with Ag only by solid-state ion exchange, AgY(SS), and (iii) SD loaded Ag exchanged zeolite, SD/AgY(SS). For comparison, solvent deposition method of SD on the parent and Ag exchanged zeolite has been also applied. Details on the preparation procedures are described below.

2.1.3. Sulfadiazine loading

The deposition of the drug in solid-state was made at room temperature by high-energy dry milling of sulfadiazine and HY or AgY(SS) in 0.8:1 weight ratio for 3 min in a DDR-GM 9458 type vibrational ball mill mixer. The resulting preparations were designated as SD/HY(SS) or SD/AgY(SS), respectively.

Sulfadiazine loading in solution was carried out in a mixture of acetone and methanol (1:1) at 37°C applying also 0.8 g of SD per 1 g support. After incubation for 24 h, the mixture was centrifuged at 15,000 rpm, rinsed with distilled water, separated by a second centrifugation and finely dried at room temperature under vacuum. Depending on the type of support, the as prepared samples were designated as SD/AgY(Sol), and SD/HY(Sol), respectively.

2.1.4. Silver loading

The Ag-exchanged Y zeolite was prepared by solid-state ion exchange (SSIE) technique in analogy to reductive SSIE procedure, widely studied formerly by our research group [31,32].

As a first step the HY powder material was homogeneously mixed with appropriate amount of $AgNO_3$, so as 4.14 mmol Ag/g zeolite Y (21.2 wt.% Ag, an amount corresponding to the calculated number of exchangeable proton sites available in the zeolite) to be intro duced. The mixing was made in the vibrational mixer for 3 min. Subsequently, a thin layer of the $AgNO_3$ + HY mixture was loaded into a Pyrex reactor, heated in dry N_2 atmosphere from room temperature to 450°C at 3°C/min for 90 min. Then the temperature was raised to 520°C and held for another 90 min. The inert gas was exchanged by air and the sample was treated at the same temperature again for 90 min. The resulting powder was designated as AgY(SS) and used for drug loading.

2.2. Methods used

X-ray powder diffraction patterns were recorded by a Philips PW 1810/3710 diffractometer with Bregg-Brentano parafocusing geometry applying monochromatized CuK_α (λ = 0.15418 nm) radiation (40 kV, 35 mA) and a proportional counter.

TEM images were taken using a MORGAGNI 268D TEM (100 kV; W filament; point-resolution = 0.5 nm) apparatus.

SEM images were prepared by a Zeiss EVO 40XVP type scanning electron microscope.

TG analysis was performed by a Setaram TG92 instrument. To follow the $AgNO_3$ degradation from the as-prepared $AgNO_3$ + HY mixture during the solid-state exchange method, heating with 3 °C/min rate up to 500°C in Ar flow was applied. The amount of loaded sulfadiazine was controlled by heating of the mixture of SD with HY or with AgY(SS) in air, at 5°C/min up to 600°C and hold up for 1 h at the same temperature.

Attenuated Total Reflection Infrared (ATR-FT-IR) spectra were recorded by means of a Varian Scimitar 2000 FT-IR spectrometer equipped with a MCT (mercury-cadmium-tellur) detector and a single reflection ATR unit (SPECAC ‘‘Golden Gate’’) with diamond ATR element. In general, 128 scans and 4 cm^{-1} resolution was applied. For all spectra ATR correction was performed (Varian ResPro 4.0 software).

2.3. Sulfadiazine in vitro release measurements

For in vitro release studies, 20 mg of the drug-loaded particles were incubated in 500 ml phosphate buffer with pH = 5.5 at 37 °C under stirring (100 rpm). At appropriate time intervals, 5 ml samples were withdrawn from the release medium, and replaced by the same

amount of fresh buffer. The concentration of the released sulfadiazine in the samples was determined by UV–VIS spectrophotometry at a wavelength of 262 nm. The concentration of sulfadiazine was calculated according to the standard curve prepared in the concentration range of 3–15 μg/ml (r = 0.996).

3. Results and discussion

It is known that the non-crystalline state of the confined drug is one of the key factors for the improvement of its dissolution [33]. Thus, we might expect that the solid-state SD encapsulation method can lead to some amorphization of the loaded drug, improving its solubility and facilitate its deposition/adsorption. In Fig. 1 the SEM pictures of the parent zeolite and its SD loaded for mulation are presented. Aggregates from smaller zeolite particles seem to be formed as a result of vibrational ball mill mixing of SD with the zeolite (Fig. 1B).

XRD analysis gives more detailed information about the crystallinity of the zeolite and SD structures (Fig. 2). In accordance with the decreased intensity of the strongest SD reflections of the grinded compound (Fig. 2A), it can be concluded that milling have led to substantial nanosizing of SD. The strongest XRD lines of the drug are clearly visible when it is deposited on the H-form of the zeolite both by solid-state or in solution (Fig. 2B). The intensity of SD reflections corresponds to the amount of loaded drug (1:0.8 = zeolite:SD ratio). In the case of solid state mixing the intensity of zeolite reflections is proportional with the amount of the zeolite in the delivery system, but it significantly decreases as a result of SD deposition in solution. Such partial crystallinity loss of the parent HY carrier not only takes place when SD is loaded by solution method (Fig. 2B), but also during the solidstate ion exchange procedure with $AgNO_3$ upon AgY(SS) preparation (Fig. 2C). The additional solid-state loading with SD over Ag-modified zeolite resulted in further amorphization of the carrier. Obviously, the intense mechanical grinding upon the subsequent solid-state encapsulation of Ag as well as of SD over the parent zeolite, results in loss of crystallinity not only for the drug but also for the zeolite carrier as the decrease of its X-ray reflections reveals (Fig. 2C).

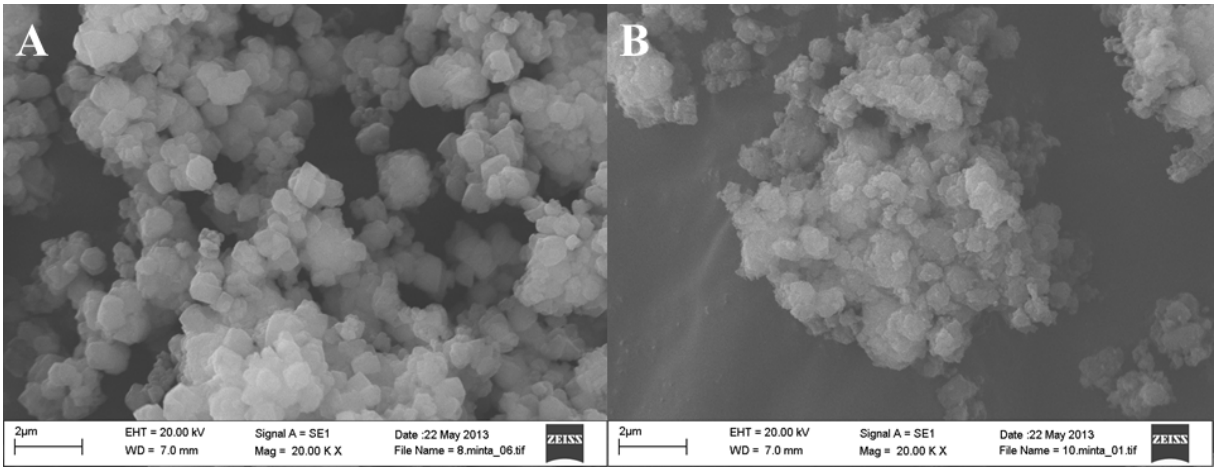

Fig. 1. SEM images of the parent HY (A) and SD/HY(SS) (B) samples

Compared to the zeolite destructive liquid SD deposition over the unmodified HY carrier, the zeolite structure does not suffer further crystallinity collapse when SD is loaded by the latter method. The almost unchanged reflections of the zeolite support, small amount of SD and formation of higher amount of AgSD, can be observed (Fig. 2C). It is possible AgSD to be also formed in SD/AgY(SS) (and not in such small amount), but invisible by XRD because of its fine distribution in the pores, in contrast to SD/AgY(Sol) in which AgSD is formed on the AgY crystallite surface.

An issue that arises here is whether the whole amount of silver supplemented in the drug system by the solid dispersion method is introduced in the zeolite framework as Ag^{+} cations, replacing the zeolite protons, or it remains on he outer zeolite surface, at least partially, as metal or oxide silver species. The XRD analysis of the Ag-containing materials (Fig. 2C) does not show any presence of such elements. This could mean that either all silver is introduced as a counter-ion or XRD invisible metal particles with a size lower than 5 nm have been formed as a result of Ag solid-state encapsulation.

TEM investigations give some indication about the state of the introduced silver. In Fig. 3 representative TEM images of AgY(SS) and the both SD loaded Ag-modifications are presented. According to the picture, metal particles have been formed on AgY(SS) surface (Fig. 3A). This means that after the applied SSIE only part of silver is kept in exchangeable positions. The remaining Ag^{+} has most probably been oxidized to Ag_2O and/or subsequently reduced to Ag^{0} upon preparation. Transformation of Ag_2O to Ag^{0} in oxidizing atmosphere has first been reported by Jacobs et al. [34] for Ag-exchanged A (LTA structure) and L zeolite dehydrated under vacuum at different temperatures. The authors found that Ag_3^{2+} clusters are

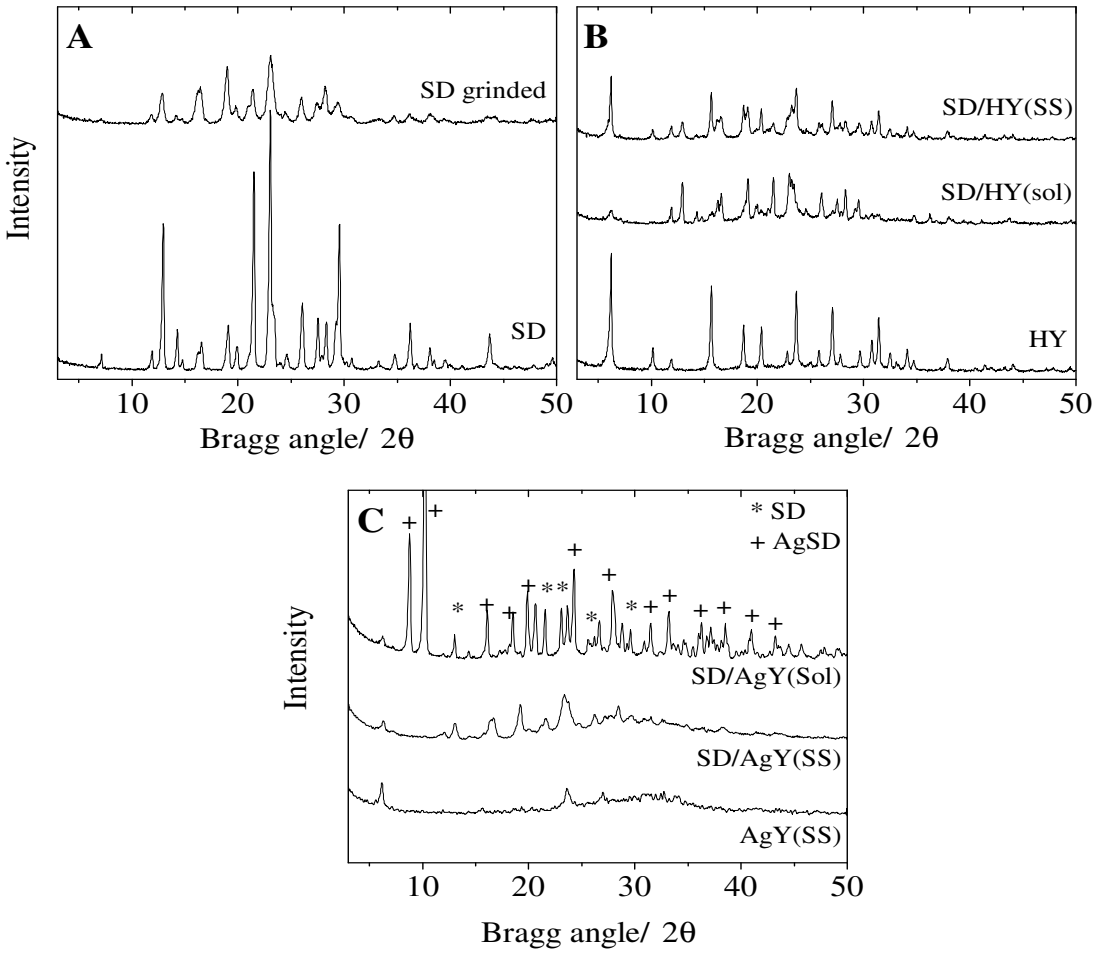

Fig. 2. XRD patterns of SD before and after grinding (A), SD/HY(Sol), SD/HY(SS) and parent HY zeolite (B), and SD loaded on AgY in solution and in solid-state (C).

stabilized in the sodalite cavities of zeolite A, but on L zeolite they seem to aggregate, originating Ag_m clusters and afterwards Ag^0 particles visible by TEM.

In case of ZSM-5 zeolite, AbuZied et al. [35] have got to the conclusion that Ag_2O and Ag^+ are simultaneously present over AgZSM-5 prepared by SSIE. The FT-IR and elemental analysis data show 95% Ag exchange level and low crystallinity Ag_2O phase detected by XRD analysis. The authors suggested the occurrence of the following reverse reaction:

$$2ZO^-H^+ + Ag_2O \leftrightarrow 2ZO^-Ag^+ + H_2O$$

generating simultaneously Ag^+ and Ag_2O nanoparticles in dependence of the temperature and the environment. Thus, one can conclude that Ag cations and metal/oxide Ag particles exist together over our AgY(SS) formulation prepared by the solid dispersion method.

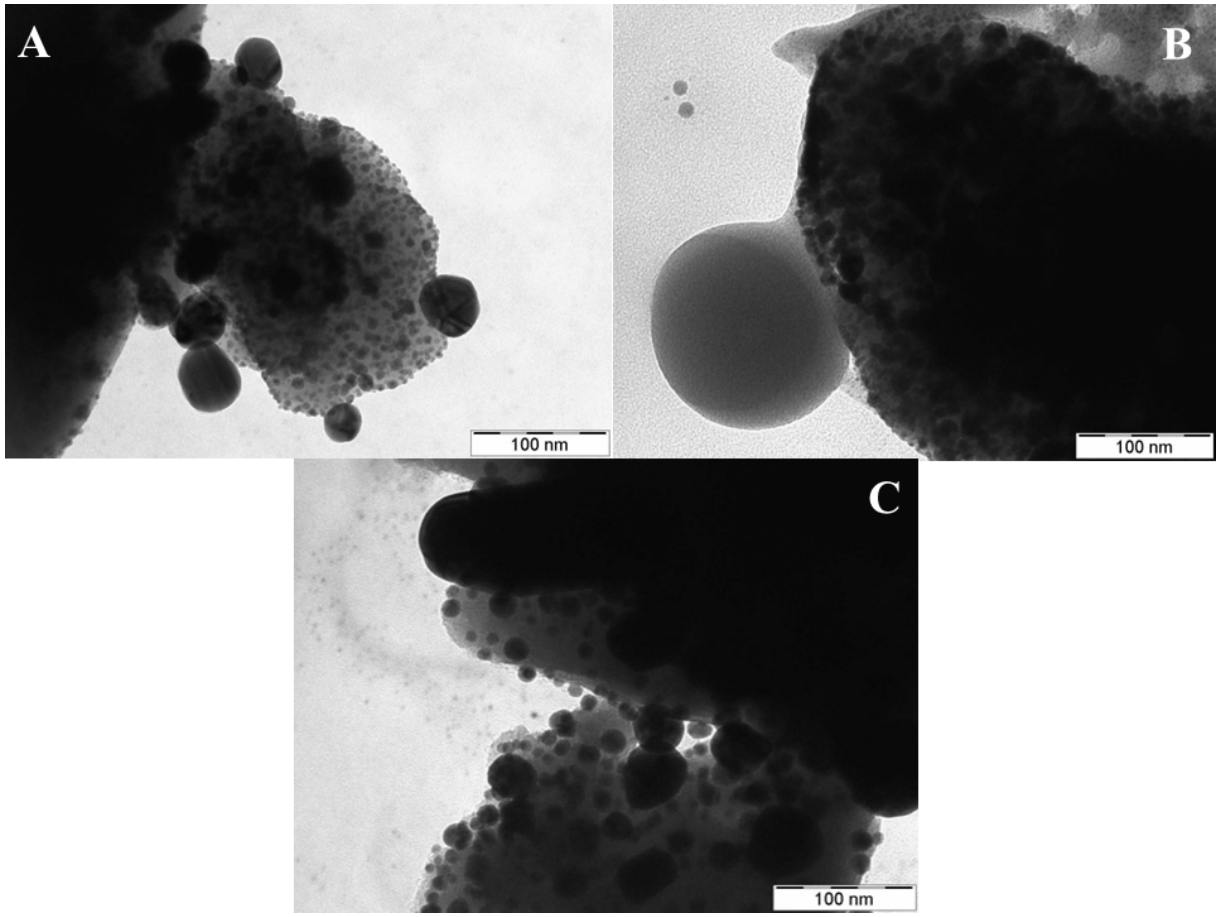

Fig. 3. TEM images of AgY(SS) (A), SD/AgY(SS) (B) and SD/AgY(Sol) (C) samples.

Small Ag nanoparticles with 5–10 nm size as well as largeraggregates (about 50 nm), are visible in Fig. 3A. However, the bigger metal particles have not been detected upon our XRD measurements. The most possible explanation of this effect is that agglomeration of silver nanoparticles upon interaction with the electron beam in the TEM apparatus has taken place in accordance with the investigations of Diaz and Mayoral [36]. The authors recommend a necessity of careful analysis of the TEM results taken from-beam sensitive materials such as silver.

Loading the Ag-zeolite with sulfadiazine by the solvent or the solid-state method does not change significantly the TEM image (Fig. 3B and C). Only overflow from melted SD crystallites with droplet shape come into view in these figures. The drug also seems to be sensitive and get melted, most probably, under the electron beam.

FT-IR spectra in the hydroxyl stretching region can prove the occurrence of an exchange reaction between the zeolite protons and silver, generating cationic silver upon the SSIE procedure.

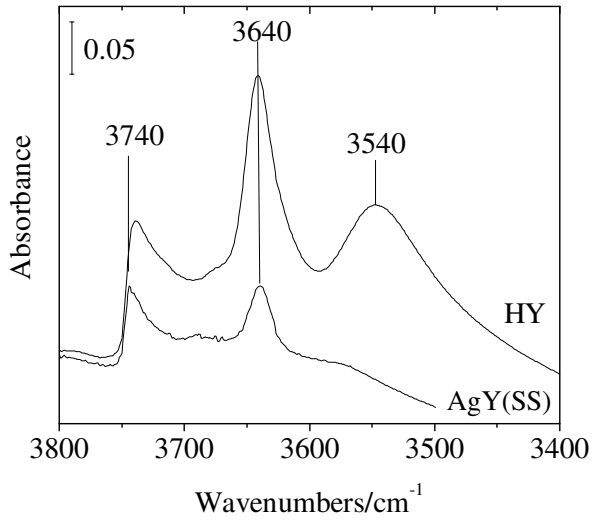

Fig. 4. FT-IR spectra of parent HY and Ag modified AgY(SS) sample, prepared by SSIE.

The observed intensity decrease of the band at 3640 cm^{-1} and the disappearance of the 3540 cm^{-1} band of the AgY(SS) sample, related to the typical low and high frequency ν(OH) stretching vibrations of Y zeolite framework [37], is an indication that such SSIE has occurred upon the high temperature treatment of $AgNO_3$ and HY mixture. It appears that a substantial part of the OH groups of the carrier has been consumed by encapsulation of Ag in cationic positions (Fig. 4).

ATR FT-IR method was also used to ascertain whether some interaction between the adsorbed SD molecules and the porous carrier, parent or Ag-modified, occurred. The spectrum of the unsupported SD reveals the characteristic stretching vibration bands of amine and sulfonamide groups in the 3500–3000 cm^{-1} range, viz. 3493–3463 cm^{-1} for the asymmetric NH_2 stretching vibration (ν_{asym}), and the symmetric one between 3390– 3359 cm^{-1} (ν_{sym}), (Fig. 5A) and also the corresponding bending frequencies (δNH_2) at 1629–1627 cm^{-1} (Fig. 5B). In respect to νNH vibration of SD, if it is adsorbed on the H^+ form of the zeolite, the stretching vibration of the formed $-NH_2^+$ group will strongly overlap with that of the amine $\nu_{sym}NH_2$, and as Braschi et al. [17] have stated, this will make difficult its precise identification. The occurrence of ionic bonding between zeolite Y and different sulfonamides including SD is thoroughly studied in the extensive research of these authors. They suppose protonation of the sulfa drug by the zeolite protons via van der Waals forces and weak H-bonding of the loaded SD and the zeolite cage surfaces. Compared to the bare SD, the $\upsilon_{asym}NH_2$ and $\upsilon_{sym}NH_2$ of SD at 3419 and 3352 cm^{-1}, respectively, are slightly shifted in our case toward higher wavenumber, i.e. to 3423 and 3355 cm^{-1} (Fig. 4B). This phenomenon is

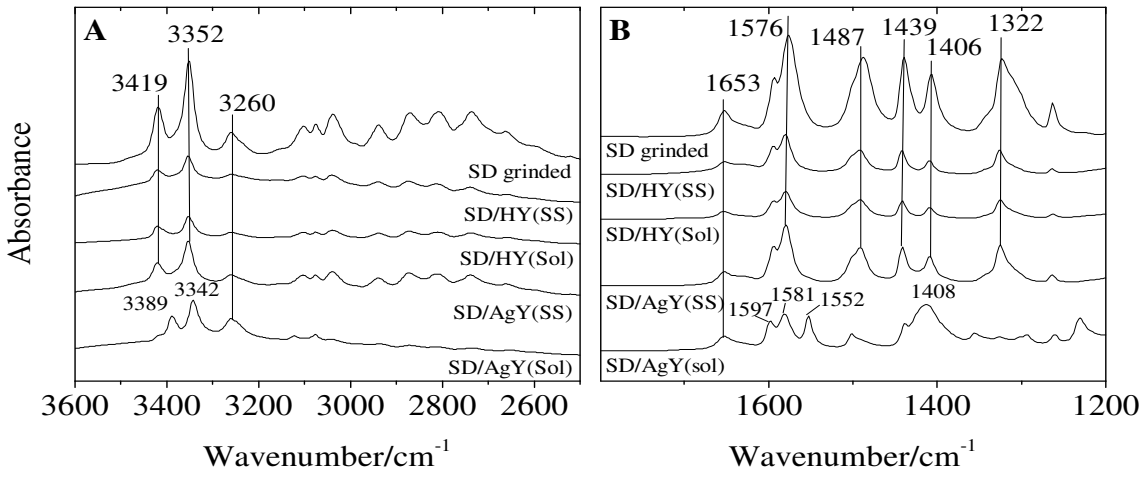

Fig. 5. FT-IR spectra of SD supported by solid or by solvent deposition method on unmodified and Ag-modified zeolite carriers in the 3500–3000 cm^{-1} region (amine and sulfonamide groups) (A), and in the NH_2 deformation, aromatic ring vibration and pyrimidine moiety (1200–1700 cm^{-1}) region (B).

opposite to the usual frequency down shift due to H-bonding. The νNH stretching assigned to 3260 cm^{-1} does not show any changes. In the case of SD/AgY(sol) sample, however, new vibration bands at 3389 and 3342 cm^{-1} come into view. The appearance of these bands is an evidence for the formation of AgSD, supported also by the XRD results.

As to the fingerprint region of the spectrum of SD, it is dominated by the NH_2 deformation at 1653 cm^{-1}, aromatic ring stretching (νCC at 1576 cm^{-1}) and bending (δCCH at 1487 cm^{-1}), and that of pyrimidine moiety (δCCH at 1439 cm^{-1} and δHCN at 1406/1408 cm^{-1}, Fig. 4C). The relative broad band around 1322 cm^{-1} can be assigned to S–O stretching.

For both HY and AgY supports, the band shift of aromatic ring and pyrimidine moiety vibrations indicates interaction of the benzene (pyrimidine) ring with the zeolite framework. For AgY sample loaded with SD by liquid deposition, moreover, bands characteristic for AgSD can be witnessed at around 1597, 1581 and 1552 cm^{-1}. The same phenomenon was experienced also in the case of SD loaded AgMCM-41 samples [29]. The band at 1552 cm^{-1} is present in the spectra of silver sulfadiazine (AgSD) compound and is assigned to the shifted ring vibrations of pyrimidine by the presence of Ag^+. The appearance of these bands can be due either to the interaction of zeolitic silver cations or metallic silver particles with the adsorbed SD resulting in the formation of AgSD. To derive AgSD was actually our intention and final goal, viz. to test the ability to get AgSD-loaded formulation overcoming the extremely low solubility of this therapeutic compound.

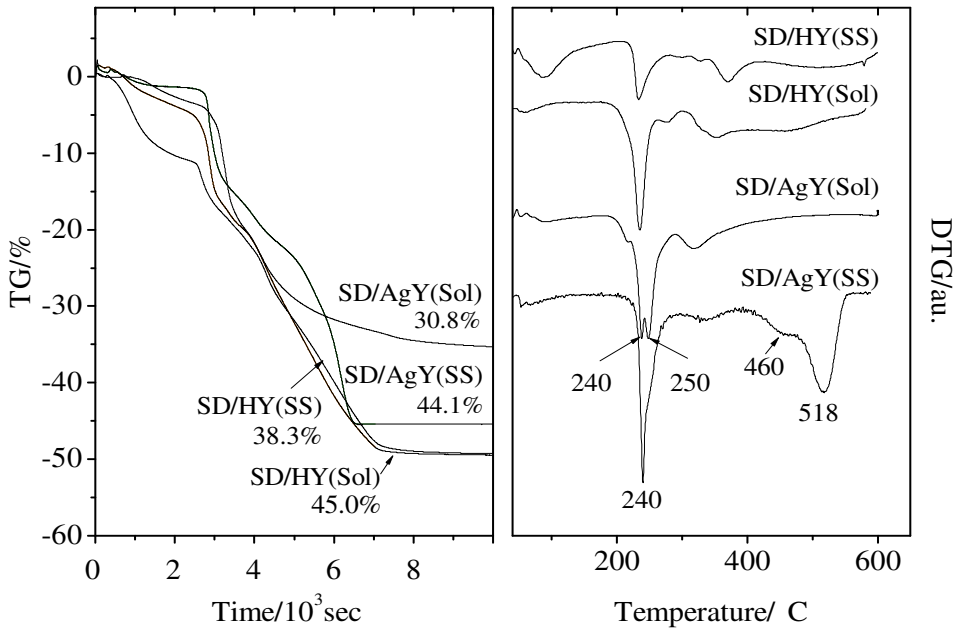

Fig. 6. TG (A) and DTG (B) profiles of SD-loaded parent and Ag-modified zeolite Y by solid dispersion and solvent deposition method.

Thermogravimetric analysis (TG) has been used to follow the decomposition of $AgNO_3$ upon the process of silver encapsulation by SSIE (not shown) as well as for quantification of the amount of loaded SD. TG analysis of the SD loaded formulations (Fig. 6) showed that with the exception of SD/AgY(Sol), the determined amount of the adsorbed drug corresponded roughly to the added amount (in 87–100%) prepared either by solid-state or by solvent method. However, only about 70% of the loaded SD is found to be adsorbed over AgY, when SD was loaded in solution (Fig. 6A). It should be noted here that comparing the DTG profiles of the drug decomposition, the low temperature peak of this sample is split (Fig. 6B) with T_{max} values of 236°C and 248°C. This also indicates that another compound that could be AgSD has been formed upon the procedure of SD deposition as a result of an ion exchange occurred between the Ag ions of the zeolite and the protons of SD. This Ag-containing product should be eliminated, together with the remaining SD, upon heating. Indeed, close decomposition maximum in the same temperature interval, differing by about 20 °C, (i.e. at 270°C and at 293°C) is observed when the individual, unsupported drugs SD and AgSD are heated at the same experimental conditions in the microbalance (not shown).

The suggestion about occurrence of ion exchange phenomena upon SD loading but only in liquid phase over the Ag-modified zeolite is in agreement with the FT-IR data (Fig. 4C) showing a band at 1552 cm^{-1} indicating formation of AgSD.

Considering the TG decomposition profiles of the SD loaded materials it could be inferred that the presence of silver on the sup- port strongly influences the interaction of the drug molecule with the zeolite carrier and respectively its way of decomposition. The TG profiles of the high temperature SD removal from the H-form of the zeolite are similar regardless of the method of its deposition, solvent or solid-state. In the case of Ag-modified carriers, however, they are quite different. When solvent deposition method is applied, the dissolved SD can react with the Ag^+ surface cations or with the Ag^+ released to the solvent. In this latter case superficial precipitation of AgSD occur on the zeolite particles and its decomposition at heating, together with that of SD, would be faster and easier (Fig. 6B).

Also, the presence of high amount of finely dispersed silver nanoparticles (see TEM results, Fig. 3) on the surface of the zeolite crystallites may block the entrances of the zeolite pore system and prevent the access of SD into it, thus reducing the adsorption capacity of this preparation. It should be noted here that when zeolite materials are used as carriers, the molecular sieve effect should not be neglected. When Ag has been incorporated into cationic framework positions, a decreased size of the zeolite channels is to be expected as well. The latter will cause, in presence of the solvent molecules in particular, diffusion restrictions for the drug occlusion. Thus, when the drug is loaded by solvent deposition method, only partial SD loading, accompanied by superficial AgSD formation would take place as also the TG curve of SD/AgY(Sol) has indicated.

Upon the first silver deposition step by solidstate ion exchange, a loss of zeolite crystallinity has occurred, which has reduced its further adsorption ability during the solvent method of SD loading. These effects could also be the reason for the observed lower amount of loaded drug (Fig. 6A), for the weaker interaction with the surface, and for the lower decomposition temperature of the active substance.

By applying the solid-state deposition method the above mentioned disadvantages can be overcome. The diffusion restrictions caused by the solvent molecules are avoided and undisturbed encapsulation of SD inside the zeolite channels might take place upon the intense mixing procedure. As a result, precipitation of AgSD on the principle of ‘‘contact-induced ion exchange’’ in the zeolite intra-crystalline water [38] can also occur. This could impede the removal of the decomposition products out of the zeolite channels as the DTG data indicates, considering the appearance of the high temperature degradation peak with T_{max} at 518°C (Fig. 6B). Naturally, upon this method of drug loading, the whole amount of added SD is available and the whole amount of degradation products removed upon heating is detected by TG (Fig. 6A). The concentration of sulfadiazine released in phosphate buffer with pH = 5.5 as a

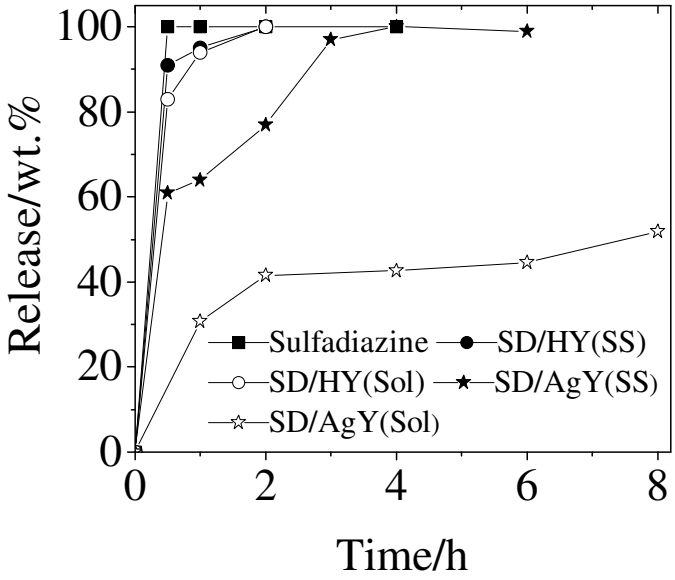

Fig. 7. Sulfadiazine release in pH = 5.5 buffer from the parent and the Ag-modified zeolite Y loaded with SD by solid dispersion and by solvent deposition method.

function of time was determined by UV–Vis spectrophotometry at a wavelength of 262 nm. The applied release media simulated the physiological conditions for release of dermatological formulations. In Fig. 7 the delivery profile of the grinded sulfadiazine substance is compared with that of SD loaded (in solid-state or in solution) parent HY zeolite as well as of its Ag-modification. As the results show, the whole amount of the unsupported grinded sulfadiazine is delivered practically immediately. A steep release (over 90% of the loaded drug) for the first hour is registered for the drug encapsulated into both preparations of the unmodified carrier. Complete SD release from the formulations with the H-form of Y zeolite was reached in 2 h.

The release profile of SD from the silver zeolites is quite different and prolonged (Fig. 7). Almost 3 h are necessary for the gradual delivery of the drug from the sample prepared by solid-state to be completed. This effect is consistent with the TGA result illustrating that much higher temperature is needed for decomposition of the loaded drug by this method. Drug occlusion into the pores of the support and stronger drug-framework silver ions interaction could be the reason for its extended release. This prolonged release of SD is similar to that of found on silver containing nanoporous silica materials [29], but much faster than on polymer based systems loaded with AgSD [39].

By SD solution deposition method over Ag-modified Y zeolite, it can be suggested that part of the silver counterions are released in the solvent and react with the drug. Thus, insoluble AgSD is precipitated on the outer surface of the support as XRD and FT-IR (Fig. 4) results

have indicated and incomplete SD release is observed for the as-prepared formulation. This could be the reason for the significantly lower quantity of SD delivered from the SD/AgY(Sol) sample during the release procedure in the buffer. Only half of the superficially loaded SD could be registered in the supernatant and the release takes longer time (Fig. 7). Therefore, the presence of silver is a key factor for the sorption ability and kinetics of delivery of this particular drug from the Ag-containing zeolite support and these characteristics strongly depend on the method of prepa- ration of the respective formulation.

Further study on the antibacterial properties would reveal the efficiency of the combined procedure for preparation of both Ag and SD encapsulated drug delivery systems. The kinetics and the amount of released silver as well as assessment of the antibacterial action of the above zeolite formulations are objects of our next studies.

4. Conclusion

Successful simplified procedure for preparation of dual Ag-sulfadiazine drug delivery system has been developed using zeolite Y as a carrier. To the best of our knowledge this is the first attempt to introduce both Ag and SD in a Y zeolite matrix by combination of solid-state ion exchange with silver and dry mill mixing with sulfadiazine.

Silver introduced into the HY carrier by solid-state ion exchange has been encapsulated in both states, viz. as Ag+ cations and as Ag^0/Ag_2O nanoparticles. The method of subsequent SD loading does not influence its release kinetics when the H-form of the zeolite is used as carrier and no noticeably sustained release can be achieved compared to pure SD. The amount of deposited SD, the nature of its interaction with the carrier as well as the release kinetics is influenced, however, by the presence of silver. These characteristics depend also on the SD loading procedure performed in solid-state or in liquid. When SD is loaded in solution, a part of the zeolite silver ions is released and interact with SD, forming AgSD and restricting the bioavailability of the formulation. By solid-state SD deposition, the reaction between the drug and the silver is limited within the limits of inter-atomic interaction, and total but prolonged drug release occurs, compared to the unmodi- fied zeolite. Thus, perspective drug release systems for topical use in burn injury can be easily prepared by the latter procedure of solid-state SD encapsulation into Ag-modified zeolite Y.

5. Acknowledgements

Financial support of the Bulgarian-Hungarian Inter-Academic Exchange Agreement is greatly acknowledged.

6. References

[1] M. Rai, K. Kon, A. Ingle, N. Duran, S. Galdiero, M. Galdiero, Appl. Microbiol. Biotechnol. 98 (2014) 1951–1961.

[2] H.V.R. Dias, K.H. Batdorf, M. Fianchini, H.V.K. Diyabalanage, S. Carnahan, R.Mulcahy, A. Rabiee, K. Nelson, L.G. Waasbergen, J. Inorg. Biochem. 100 (2006)158–160.

[3] L. Balogh, D.R. Swanson, D. Tomalia, G.L. Hagnauer, A.T. McManus, Nano Lett. 1 (2001) 18–21.

[4] M. Ramstedt, N. Cheng, O. Azzaroni, D. Mossialos, H.J. Mathieu, W.T.S. Huck, Langmuir 23 (2007) 3314–3321.

[5] V. Sambhi, M.M. MacBride, B.R. Peterson, A. Sen, J. Am. Chem. Soc. 128 (2006) 9798–9808.

[6] Z. Shi, K.G. Neoh, E.T. Kang, Langmuir 20 (2004) 6847–6852.

[7] S.R. Bonde, D.P. Rathod, A.P. Ingle, R.B. Ade, A.K. Gade, M.K. Rai, Nanosci. Meth. 1 (2012) 25–36.

[8] R.M.E. Richards, R.B. Taylor, D.K.L. Xing, J. Pharm. Sci. 80 (1991) 861–867.

[9] R.M.E. Richards, D.K.L. Xing, Int. J. Pharm. 75 (1991) 81–87.

[10] M. Potara, E. Jakab, A. Damert, O. Popescu, V. Canpean, S. Astilean, Nanotechnology 22 (2011) 135101–135109.

[11] P. Li, J. Li, C. Wu, Q. Wu, J. Li, Nanotechnology 16 (2005) 1912–1917.

[12] P. Payra, P.K. Dutta, in: S.M. Auerbach, K.A. Carrado, P.K. Dutta (Eds.), Handbook of Zeolite Science and Technology, Dekker, New York, 2004, pp.1–19.

[13] A. Dyer, S. Morgan, P. Wells, C. Williams, J. Helminthol. 74 (2000) 137–141.

[14] K.A. Fisher, K.D. Huddersman, M.J. Taylor, Chem. Eur. J. 9 (2003) 5873–5878.

[15] J. Galownia, J. Martin, M.E. Davis, Microporous Mesoporous Mater. 92 (2006) 61–63.

[16] H. Zhang, Y. Kim, P.K. Dutta, Microporous Mesoporous Mater. 88 (2006) 312–318.

[17] I. Braschi, G. Gatti, G. Paul, C.E. Gessa, M. Cossi, L. Marchese, Langmuir 26 (2010) 9524–9532.

[18] I. Braschi, S. Blasioli, L. Gigli, C.E. Gessa, A. Alberti, A. Martucci, J. Hazard. Mater. 178 (2010) 218–225.

[19] I. Braschi, G. Paul, G. Gatti, M. Cossi, L. Marchese, RSC Adv. 3 (2013) 7427–7437.

[20] Z. Popovich, M. Otter, G. Calzaferri, L. De Cola, Angew. Chem. Int. Ed. 46 (2007) 6188–6191.

[21] C.A. Strassert, M. Otter, R.Q. Albuquerque, A. Hone, Y. Vida, B. Maier, L. De Cola, Angew. Chem. Int. Ed. 48 (2009) 7928–7931.

[22] E. Merisko-Liversidge, G. Liversidge, E. Cooper, Eur. J. Pharm. Sci. 18 (2003) 113–120.

[23] C. Keck, S. Kobierski, R. Mauludin, R. Muller, Dosis 24 (2008) 124–128.

[24] D.G. Fatouros, D. Douroumis, V. Nikolakis, S. Ntais, A.M. Moschovi, V. Trivedi, B. Khima, M. Roldo, H. Nazar, P.A. Cox, J. Mater. Chem. 21 (2011) 7789–7796.

[25] S.-C. Shen, W.K. Ng, L. Chia, J. Hu, R.B.H. Tan, Int. J. Pharm. 410 (2011) 188–195.

[26] R. Mellaerts, J. Jammaer, M. van Speybroeck, H. Chen, J. van Humbeeck, P. Augustijns, G. van den Mooter, J. Martens, Langmuir 24 (2008) 8651–8659.

[27] M. Popova, K. Yoncheva, A. Szegedi, Y. Kalvachev, N. Benbassat, V. Mavrodinova, Bulg. Chem. Commun. 46A (2014) 117–122.

[28] M. Popova, A. Szegedi, V. Mavrodinova, N. Novak Tušar, J. Mihály, S. Klébert, N. Benbassat, K. Yoncheva, J. Solid. State Chem. 219 (2014) 37–42.

[29] A. Szegedi, M. Popova, K. Yoncheva, J. Makk, J. Mihály, P. Denkova, J. Mater. Chem. B 2 (2014) 6283–6292.

[30] C.L. Fox Jr., U.S. pat. 3,761,590 (1973).

[31] V. Mavrodinova, M. Popova, R.M. Mihályi, G. Pál-Borbély, Ch. Minchev, Appl. Catal. A: Gen. 248 (2003) 197–209.

[32] V. Mavrodinova, M. Popova, R.M. Mihályi, G. Pál-Borbély, Ch. Minchev, Appl. Catal. A 262 (2004) 78–83.

[33] B. Hancock, M. Parks, Pharm. Res. 17 (2000) 397–404.

[34] P.A. Jacobs, J.B. Uytterhoeven, J. Chem. Soc.-Farad. Trans. I (75) (1979) 56–64.

[35] B.M. Abu-Zied, W. Schwieger, A. Unger, Appl. Catal. B: Environ. 84 (2008) 277–288.

[36] I. Diaz, A. Mayoral, Micron 42 (2011) 512–527.

[37] A.K. Sen, G. Singh, K. Singh, R.N. Handa, S.N. Dubey, P.J. Squattrito, Proc. Indian Acad. Sci. Chem. Sci. 110 (1998) 75–81.

[38] G. Borbely, H. Beyer, L. Radics, P. Sandor, H. Karge, Zeolites 9 (1989) 428–431.

[39] Y.S. Cho, J.W. Lee, J.S. Lee, J.H. Lee, T.R. Yoon, Y. Kuroyanagi, M.H. Park, D.G. Pyun, H.J. Kim, J. Mater. Sci. Mater. Med. 13 (2002) 861–865.